



Astronomical constraints on the duration of the early Jurassic Hettangian stage and recovery rates following the end-Triassic mass extinction (St Audrie's Bay/East Quantoxhead, UK)

M. Ruhl ^{a,*}, M.H.L. Deenen ^b, H.A. Abels ^c, N.R. Bonis ^a, W. Krijgsman ^b, W.M. Kürschner ^a

^a Laboratory of Palaeobotany and Palynology, Institute of Environmental Biology, Utrecht University, Budapestlaan 4, NL-3584 CD Utrecht, The Netherlands

^b Paleomagnetic Laboratory Fort Hoofdijk, Department of Earth Sciences, Utrecht University, Budapestlaan 17, 3584 CD Utrecht, The Netherlands

^c Stratigraphy and Paleontology, Faculty of Geosciences, Utrecht University, P.O. box 80021, 3508 TA, Utrecht, The Netherlands

ARTICLE INFO

Article history:

Received 28 October 2009

Received in revised form 22 March 2010

Accepted 5 April 2010

Available online 10 May 2010

Editor: P. DeMenocal

Keywords:

Triassic
Jurassic
cyclostratigraphy
astronomical
carbon isotope
Hettangian
mass extinction
recovery

ABSTRACT

The end-Triassic environmental crisis with major extinctions in the marine realm is followed by successive recovery in the lower Jurassic Hettangian Stage. Accurate timing of events is however still poorly constrained. In this study, combined field observations and physical and chemical proxy records, covering the uppermost Triassic and lower Jurassic marine successions of St Audrie's Bay and East Quantoxhead (UK), have been used to construct a floating astronomical time-scale of ~2.5 Myr in length. This time-scale is based on the recognition of meters thick cycles in limestone and (black) shale predominance and concurrent variability in physical and chemical proxy records. Three to five individual black-shale beds occur within these meter-scale sedimentary bundles and are interpreted to reflect precession-controlled changes in monsoon intensity, while the bundles are interpreted as forced by the ~100-kyr eccentricity cycle. On the basis of these findings, we propose an astronomically constrained duration of the Hettangian stage of 1.8 Myr in the UK and unequal duration of Hettangian ammonite zones (*Psiloceras planorbis* zone: ~250 kyr; *Alsatites liasicus* zone: ~750 kyr; *Schlotheimia angulata* zone: ~800 kyr). Within this astronomical framework, the extinction interval and coinciding negative CIE represent 1 to 2 precession cycles (~20–40 kyr). The amount of time succeeding the end-Triassic negative carbon isotope excursion (CIE) and preceding the first Jurassic ammonite occurrence (in the UK) is constrained to 6 climatic precession cycles (~120 kyr). Cyclostratigraphic correlation to the astronomically-tuned sedimentary record of the continental Newark basin (USA) allows to locate the stratigraphic position of the marine defined Triassic–Jurassic and Hettangian–Sinemurian boundary in the continental realm. Continuous low $\delta^{13}\text{C}_{\text{TOC}}$ values throughout the Hettangian and early Sinemurian, succeeding volcanic activity in the Central Atlantic Magmatic Province (CAMP), may suggest a long-term change in Earth's global biogeochemical cycles, which do not fully recover for several million years.

© 2010 Elsevier B.V. All rights reserved.

1. Introduction

The end-Triassic biosphere experienced a severe environmental crisis with major extinctions in the marine realm (Raup and Sepkoski, 1982), pronounced changes in terrestrial ecosystems (Olsen et al., 2002; McElwain et al., 2009), and large turnovers in global biogeochemical cycles (Hesselbo et al., 2002), all possibly related to the onset of Central Atlantic Magmatic Province (CAMP) volcanism (Deenen et al., 2010). Large parts of Jurassic chronostratigraphy, including the Triassic–Jurassic (T–J) boundary, are based on north-west European ammonite biochronology (Pálfy, 2008). However, estimates on absolute ages for the base of the Jurassic period and the

duration of lower Jurassic stages largely vary between studies. An accurate geological time-scale is of crucial importance to effectively integrate temporal data from different geological disciplines (e.g. stratigraphy, palaeontology, geochemistry, geophysics) and to allow for detailed correlations between key-outcrops of the T–J boundary interval. Independent time constraints allow to better confine the pace of geological processes (e.g. sedimentation rate, plate velocity, subsidence/uplift rates) and are of particular importance for understanding recovery rates of ecosystems and biota after the end-Triassic mass extinction.

We studied an ~120 m long, marine sedimentary sequence in St Audrie's Bay and East Quantoxhead (UK, Fig. 1), which includes the Global boundary Stratotype Section and Point (GSSP) for the base of the Sinemurian stage (Bloos and Page, 2002). The studied upper Rhaetian (latest Triassic) to lower Sinemurian (early Jurassic) time interval covers the complete Hettangian stage in the UK and

* Corresponding author.

E-mail address: m.ruhl@uu.nl (M. Ruhl).

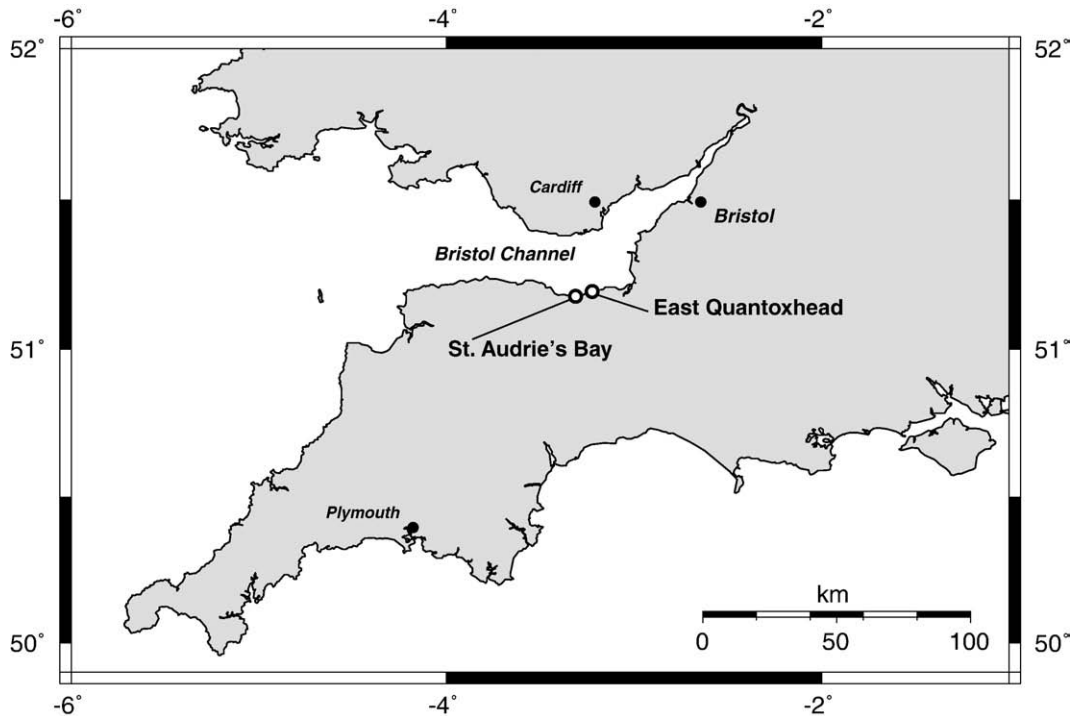


Fig. 1. The studied St Audrie's Bay ($51^{\circ}10'54.70''\text{N}/3^{\circ}17'09.79''\text{W}$) and East Quantoxhead ($51^{\circ}11'27.91''\text{N}/3^{\circ}14'12.25''\text{W}$) outcrops are located in southwest England along the Somerset coastline, on the south coast of the Bristol Channel.

comprises the end-Triassic mass extinction and subsequent lower Jurassic recovery interval (Warrington et al., 2008). The lack of lava flows and ash layers in the north Somerset coastal region makes the use of radiometric dating techniques impossible. We propose to assign astronomical parameters to observed oscillations in lithology and physical and chemical proxy records. This approach provides cyclostratigraphic time constraints on (i) the pace of lower Jurassic recovery rates, (ii) the duration of the Hettangian stage, and (iii) the duration of Hettangian ammonite zones. We tune the biostratigraphically well-constrained lower Jurassic marine proxy records to the astronomically-tuned geomagnetic polarity time-scale (GPTS) of the continental Newark basin and we discuss the duration of perturbations in the $\delta^{13}\text{C}_{\text{TOC}}$ signature in relation to volcanic emissions in the Central Atlantic Magmatic Province.

2. Geological background

2.1. Chronostratigraphy

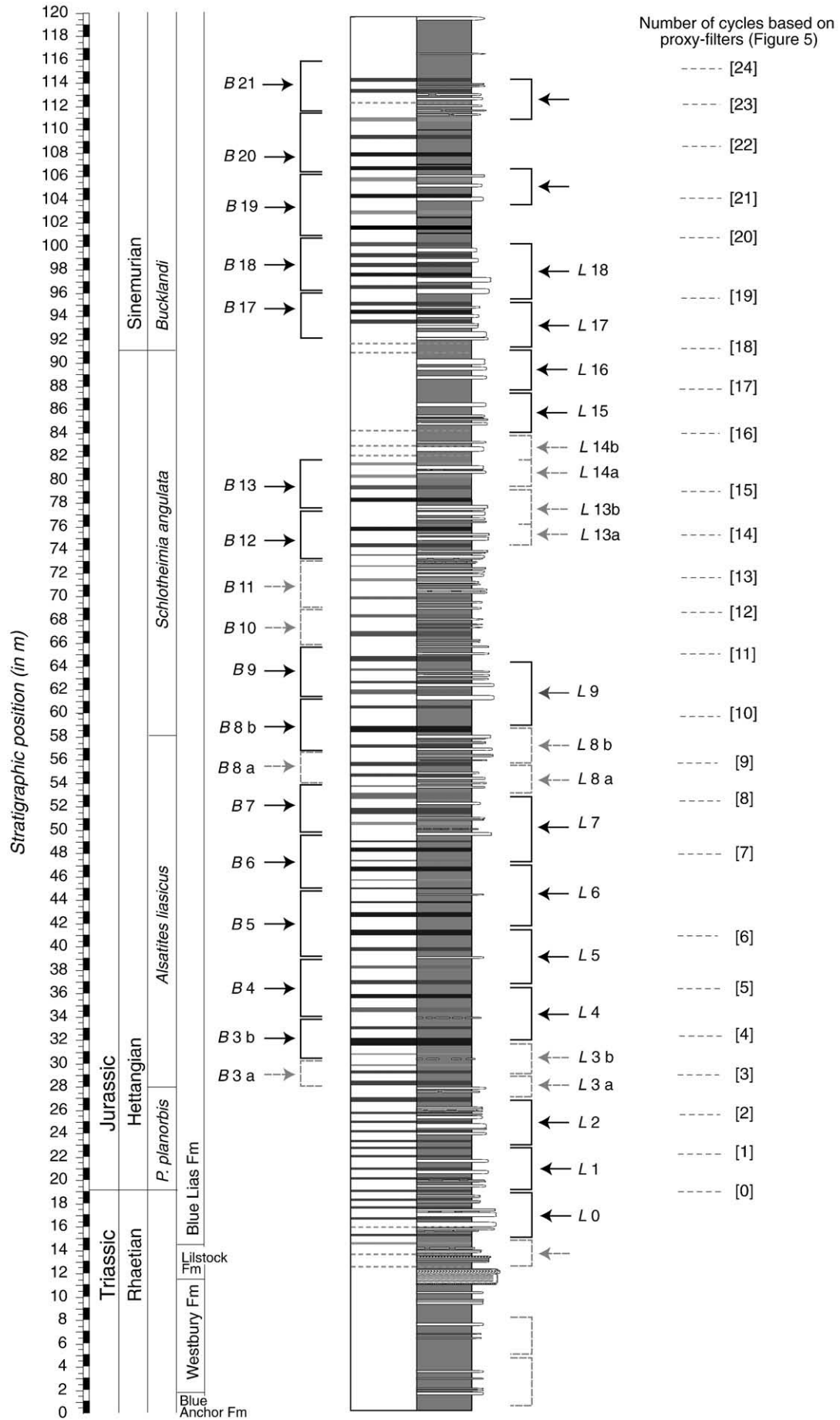
Absolute age estimates for the T–J boundary evolved from ~ 192 Ma (Van Hinte, 1976), to ~ 208 Ma (Kent and Gradstein, 1985), ~ 212.5 Ma (Bayer, 1987) and ~ 199.6 Ma (Pálffy et al., 2000). Contradicting dating results in this time interval may be caused by the use of different (isotopic) chronometers. For example, the latest Rhaetian in the Argana basin and the High Atlas (Morocco) is $^{40}\text{Ar}/^{39}\text{Ar}$ dated between ~ 200.3 and 198.0 Ma (Marzoli et al., 2004) and it is U–Pb and Pb/Pb dated at ~ 201.27 – 201.48 Ma and 203.97 Ma, respectively, in the Fundy basin (Schoene et al., 2006). The duration of the Hettangian was previously estimated at ~ 4 Myr (Kent and Gradstein, 1985) and ~ 9 Myr (Haq et al., 1987; 1988). With increased availability of radiometric dating methods, its duration decreased to ~ 3.1 Myr in the GTS2004 (Gradstein et al., 2004). Most recent constraints on latest Rhaetian ($\sim 201.58 \pm 0.28$ Ma) and uppermost Hettangian ($\sim 199.53 \pm 0.29$ Ma) ages are based on zircon U–Pb dating (Schaltegger et al., 2008) of ash layers in the marine Pucara basin (Ucubamba valley, northern Peru) and indicate a duration of the Hettangian between ~ 1.48 and ~ 2.62 Myr. Cyclostratigraphic estimates of ~ 2.4 Myr for the Hartford sequence, which extends into

the Sinemurian (Hartford basin, USA; Kent and Olsen, 2008), and magnetostratigraphic correlation to the Paris basin Montcornet core (Yang et al., 1996) support a duration of the Hettangian stage of only a few million years.

2.2. Palaeoenvironment and biostratigraphy

The upper Triassic Blue Anchor, Westbury and Lillstock Formations (Fm) in the UK, are succeeded by the uppermost Rhaetian and lower Jurassic Blue Lias Fm, which covers the Hettangian stage and continues well into the Sinemurian. The Williton Mb (Blue Anchor Fm; Fig. 2) was deposited in a shallow marine environment (Warrington et al., 2008). Fluctuations in relative sea level likely controlled the distribution of facies from the succeeding Westbury Fm (Hesselbo et al., 2004). The transition from the Westbury to Lillstock Fm (lower Cotham Mb) may reflect subsequent shallowing of the depositional environment from upper shelf to peritidal water depths (Wignall and Bond, 2008). The (syn-sedimentary) deformed limestone beds (0.5 m thick) in the middle of the Cotham Mb are followed by an erosional surface, which may indicate a short temporary emergence (Hallam and Wignall, 1999; Hesselbo et al., 2004; Warrington et al., 2008). The following upper Cotham Mb may represent a coastal environment (Mander et al., 2008) with a flooding surface at the Cotham to Langport Mb transition (Hesselbo et al., 2004). The Langport Mb (Lillstock Fm) was deposited either in a shallow lagoonal environment in a broad and shallow seaway (Warrington et al., 2008), or during sea-level rise on a carbonate ramp (Hesselbo et al., 2004). Sea-level change at the Lillstock to Blue Lias Fm transition is disputed with either a sea-level fall (Wignall and Bond, 2008) or a sea-level rise and the final drowning of the carbonate platform (Hesselbo et al., 2004). The sedimentary basin was surrounded by partly emerged platforms (Radley, 2008). The lower Jurassic Blue Lias Fm was deposited during a phase of rapid flooding allowing the development of laminated, organic-rich shales (Hallam, 1995, 1997; Warrington et al., 2008).

The Blue Lias Fm has been subject to extensive bio-, chrono- and chemostratigraphic studies (Hallam, 1987; Smith, 1989; McRoberts



and Newton, 1995; Weedon et al., 1999; Hesselbo et al., 2002; Deconinck et al., 2003; Hounslow et al., 2004; Mander and Twitchett, 2008; Warrington et al., 2008; Korte et al., 2009). The most important outcrops are located in the Lyme and Dorset regions (southwest coast, UK) and the northern Somerset coast (this study, Fig. 1). The T–J boundary section at St Audrie's Bay (51°10'54.70"N/3°17'09.79"W) was previously proposed as GSSP for the base of the Jurassic (Warrington et al., 1994, 2008) with the first occurrence (FO) of the ammonite *Psiloceras planorbis* in the basal part of the Blue Lias Fm as principal boundary marker (Warrington et al., 2008). The slightly lower FO of *Cerebropollenites thiergartii* pollen may represent a terrestrial marker for the base of the Jurassic in this section (Bonis et al., in press). Recently, the Kuhjoch section (Austria) (Hillebrandt et al., 2007) was accepted as T–J boundary GSSP by voting of the IGS (Morton, 2008a,b). Both the FO of *C. thiergartii* pollen as distinct shifts in organic C-isotope records may be used for stratigraphic correlation between St Audrie's Bay and the T–J boundary GSSP. Comparison of the stratigraphic position of the T–J boundary in the Pucara basin (Peru) and the European sections is based on ammonite stratigraphy, with the last occurrence of *Choristoceras marshi* and *Choristoceras crickmayi* and the subsequent FO of *Psiloceras spelae* marking the T–J boundary (Schaltegger et al., 2008).

The East Quantoxhead outcrop (51°11'27.91"N/3°14'12.25"W) is located 3 km east of St Audrie's Bay at Limekiln Steps. The Blue Lias Fm in this section contains the GSSP for the base of the Sinemurian (Bloos and Page, 2002).

2.3. Lithology

The sedimentary sequence of the Blue Lias Fm in the St Audrie's Bay and East Quantoxhead sections is marked by distinct alternations of homogeneous and inhomogeneous limestone beds and marls to shales. Limestone beds are mostly impure micrite mud- to wackestones and are 10 to 20 cm thick with extremes up to 50 cm. The limestone facies consists of fine-grained, predominantly clay-grade sediments containing varying proportions of siliciclastic clay minerals and micrite (Paul et al., 2008). They are suggested to have settled primarily from suspension without any subsequent disturbance (Weedon, 1985/86). Some of the limestone beds have been diagenetically altered by redistribution of calcium-carbonate cement (Campos and Hallam, 1979; Hallam, 1986; Paul et al., 2008) with prolonged sulphate reduction and pyrite formation (Bottrell and Raiswell, 1989). This process led pale marls to cement into hard limestone beds that show an irregular lateral distribution.

Limestones are interspersed by siliciclastic marl and shale intervals, which are a few centimeters up to several meters in thickness. These beds mainly consist of pale-grey marls, dark-grey marls and organic-rich laminated black-shales (Paul et al., 2008). Siliciclastic sediments consist of (land-derived) clay minerals and marine and terrestrial organic matter (Weedon 1985/86).

Sedimentary rhythms in the Blue Lias Fm consist of a laminated black-shale that grades into a dark-grey marl, and a pale-grey marl commonly with concretionary to tabular (cemented) micritic limestone, which on top turns back into dark-grey marls and shales (Paul et al., 2008). These rhythms appear not always symmetrical because (organic-rich) shales or marls/limestones did not always develop or carbonate-rich sediments were diagenetically altered. Also the number of indurated limestone beds is significantly different from the number of sedimentary rhythms, due to the differential secondary cementation (e.g. Paul et al., 2008). The origin of the rhythmic

sedimentation has been matter of debate (Campos and Hallam, 1979; Weedon, 1985/86; Hallam, 1986; Bottrell and Raiswell, 1989; Smith, 1989; Paul et al., 2008), with orbital climate forcing as a potential mechanism. The rhythmic alternations of lithologies were suggested to represent ~20-kyr precession cycles while bundles of structurally different limestone beds resulted from harmonics between the ~20-kyr precession and ~40-kyr obliquity (based on magnetic susceptibility records from Lyme Regis; Weedon et al., 1999) or ~100-kyr eccentricity forcing (Paul et al., 2008). Distinct limestone-shale couplets in these sections are recognized over tens of kilometers suggesting chronostratigraphic significance and a stable allogenic forcing mechanism likely to be high-frequency climate control (Weedon, 1985/86; Smith, 1989). Previous cyclostratigraphic studies were however performed on sections that were shown to contain minor to major sedimentary discontinuities.

3. Methods

Field expeditions to the St Audrie's Bay (SAB) and East Quantoxhead (EQH) outcrops were undertaken in 2007, 2008 and 2009. An ~10 m stratigraphic overlap between both localities is observed through characteristic patterns of alternating limestone-shale sequences (Whittaker and Green, 1983). Over 700 samples were collected from an ~108 m interval (10–15 cm resolution) comprising the Rhaetian Lilstock Fm and the Rhaetian, Hettangian and lower Sinemurian part of the Blue Lias Fm. The marly to silty sediments and shales were studied for several chemical and physical proxy markers (CaCO₃: 394 samples/109.5 m; total organic carbon (TOC) content: 332 samples/94 m; magnetic susceptibility (MS): 738 samples/109.5 m). The $\delta^{13}\text{C}_{\text{TOC}}$ record of Hesselbo et al. (2002) was extended upwards with 317 samples (91.13 m) and with a 2.4 m (14 samples) overlap. The indurated limestones were not sampled for these proxies.

A 10–15 cm resolution magnetic susceptibility record was measured on crushed and freeze-dried silty to marly sediments from the top of the Rhaetian Westbury and Lilstock Fm well into the Hettangian and Sinemurian Blue Lias Fm (Fig. 5). Measurements were performed with a KLY-2 Susceptometer at the Paleomagnetic Laboratory 'Fort Hoofddijk,' Utrecht University, The Netherlands. The presented values of each sample are weight-corrected averages of at least three measurements.

The calcium-carbonate content was measured on 20–30 cm resolution within the shale intervals (Fig. 5). The weight-percentage of calcium-carbonate in a dry sample is represented by the weight loss of the sample after acid dissolution. About 0.9 g of powdered sediment was rinsed twice with 15 ml of 1 M HCl. To reach almost neutral pH values, the residue was additionally rinsed twice with 22.5 ml demineralized water and subsequently freeze-dried.

The total organic carbon (TOC) content was measured on 20–30 cm resolution on the Hettangian (starting in the upper *P. planorbis* zone) and Sinemurian marls and shales from the Blue Lias Fm (Fig. 5). The carbon content of around 9 mg of homogenized de-carbonated sample residue was analyzed online on a CNS-analyzer (NA 1500) following standard procedures, at the Department of Earth Sciences, Utrecht University. The TOC content of the sediment was calculated by multiplying the carbon content of the de-carbonated sample by the ratio between the weight of the de-carbonated sample and the original weight of the sample.

The $\delta^{13}\text{C}_{\text{TOC}}$ values were measured on ~20–30 cm resolution, on the same samples as the TOC measurements, starting at 26.10 m from the base of the Hesselbo et al. (2002) C-isotope curve and covering

Fig. 2. Lithological representation of the combined St Audrie's Bay and East Quantoxhead sections based on field observations and with stratigraphic position in meters. The studied stratigraphic sequence covers the upper Triassic (Rhaetian) to lower Jurassic (Hettangian and base Sinemurian). The assigned bundles on the right reflect changes in limestone predominance (*L* numbers) and on the left reflect changes in black-shale predominance (*B* numbers). The [numbers] on the far right reflect the stratigraphic position of maxima in the eccentricity filters of proxy data (see Fig. 5).



Fig. 3. Cliff-face overview of the St Audrie's Bay section covering the T–J boundary and most of the Hettangian. Continuous black lines reflect ~100-kyr eccentricity cycles (based on field observations and filtered proxy data).

most of the Hettangian and lower Sinemurian. Bulk organic C-isotope values were measured on homogenized de-carbonated sample residue, using ~30 µg of carbon, by Elemental Analyzer Continuous Flow Isotope Ratio Mass Spectrometry using a Fisons 1500 NCS Elemental Analyzer coupled to a Finnigan Mat Delta Plus mass spectrometer at the Geochemistry group of the Department of Earth Sciences, Utrecht University. Isotope ratios are reported in standard delta notation relative to Vienna PDB. Analytical precision based on routine analysis of two internal laboratory standards for every ten samples indicated a standard deviation of 0.06‰.

Frequency analysis was performed on all proxy records with the AnalySeries program, edition 1.1.1 by Paillard et al. (1996). Data were linearly detrended before using the Blackman–Tuckey method (compromise predefined level, Bartlett window). Power spectra (with a 90% confidence interval) of each proxy are reported in cycles/cm.

4. Results

4.1. Lithologic trends

The upper Triassic and lower Jurassic sedimentary succession is marked by pronounced changes in lithology on a larger scale than the basic sedimentary rhythms discussed in Section 2.3 (Figs. 2 and 3). The top of the Blue Anchor and the Westbury Fm are mainly represented by marly to silty shales (Fig. 2). The succeeding Lilstock and lower part of the Blue Lias Fm (up to 26.5 m) and the upper Hettangian *Schlotheimia angulata* zone are marked by (indurated) limestone predominance (Fig. 2). Most of the Hettangian *Alsatites liasicus* and Sinemurian *Bucklandi* zones are again represented by marl/shale deposition.

4.1.1. Periodic oscillations in limestone predominance

A detailed lithological representation of the St Audrie's Bay and East Quantoxhead outcrops (Fig. 2) reveals periodic changes in limestone predominance and distinct bundles of limestone beds, at a similar scale to the bundles recognized by Smith (1989). These bundles are observed in most of the Hettangian and lower Sinemurian and arbitrarily numbered L0 to L18 (Fig. 2). They vary in thickness between ~3–4 m in limestone-dominated intervals and ~5 m in shale-dominated intervals. Cyclic variations in limestone bed predominance are best observed in the lower Hettangian (L0 to L9) and the Hettangian–Sinemurian transition (L15 to L18). Bundling of limestone beds is less clear in the limestone-dominated interval between 64.5 and 84 m (Fig. 2). Field observations suggest that bundles L13-a/b and L14-a/b are potentially four separate bundles, similar to bundles L3a, L3b, L8a and L8b. The amount of individual limestone beds per bundle varies throughout the section. Most of the middle Hettangian *A. liasicus* zone (bundles L3 to L6) is marked by only one limestone bed per bundle, in contrast to the T–J transition and the upper Hettangian where one bundle contains up to 8 to 10 limestone beds.

4.1.2. Periodic oscillations in black-shale predominance

The lithological representation of the Blue Lias succession also reveals pronounced changes in organic matter content, represented by e.g. distinct color changes within the siliciclastic facies (Figs. 2 and 4). In the idealized sedimentary rhythm, pale-grey marls alternate with distinctly dark-grey to black, often laminated, organic-rich shales every ~60 to 100 cm. On a larger scale, 1–2 pronounced black-shale beds (tens of centimeters thick) alternate with two to three less-developed black-shales. Such bundles of 3 to 5 black-shale horizons are observed throughout the Hettangian (Fig. 4) and lower Sinemurian and vary in thickness similar to the limestone bundles. In Fig. 2, these bundles are tentatively numbered B3 to B21. The bundles are most pronounced in the *A. liasicus* zone (B3–B8) and lowermost

Sinemurian, and less-pronounced in the uppermost Rhaetian and uppermost Hettangian (Fig. 2). Black-shales do occur in bundles B3, B10 and B11, but bundling of these beds is less straightforward.

4.1.3. Periodic oscillations in limestone and black-shale predominance

Comparison of the recognized bundles in limestone and black-shale occurrence reveals that these co-occur in opposite phase relationship (Fig. 2). This is most clear for bundles B4 to B9 with bundles L4 to L9, in which B8 and L8 both are less certain bundles. Altogether, bundles consist of a limestone-dominated and a shale-dominated interval. These bundles of limestone beds and black-shales vary in thickness throughout the sedimentary sequence. On average both the limestone and the black-shale bundles are around 4 m in thickness, with thicker bundles occurring in shale-dominated intervals and thinner bundles in the limestone-dominated intervals. The distance between individual black-shale horizons varies positively relative to the thickness of the assigned bundles. Based on field observations, we count a minimum of 16 and a maximum of 20 bundles of limestone beds and black-shales in the Hettangian, which reflect periodic changes in limestone and black-shale predominance, and 59 individual black-shales. Two bundles, L15 and L16, do not contain any black-shales leaving 14 (and up to 18) bundles with 4.2 (and down to 3.2) individual black-shales on average (Fig. 2).

4.2. Chemical and physical proxy records

The $\delta^{13}\text{C}_{\text{TOC}}$ record shows meter-scale fluctuations of ~2‰ around a –29‰ Hettangian and lower Sinemurian average (Fig. 5). These values show, similar to lower Jurassic C-isotope data of Hesselbo et al. (2002), an ~2.5‰ negative offset relative to Rhaetian average values (Fig. 5). Smaller amplitude oscillations at higher frequency (~0.5–1.5‰; ~80 cm), superimposed on the large-scale fluctuations, often coincide with individual black-shale horizons (Fig. 5). Not all black-shale events are, however, recognized in the $\delta^{13}\text{C}_{\text{TOC}}$ record due to too low sample resolution of the latter. The total organic carbon (TOC), calcium-carbonate (CaCO_3) and magnetic susceptibility (MS) records are all marked by similar small-scale (~80 cm) oscillations superimposed on larger meter-scale fluctuations (Fig. 5). Fluctuations in TOC content, varying between almost 0 and 6% with peaks up to 10%, mainly occur in the shale-dominated Hettangian *A. liasicus* zone and Sinemurian *Bucklandi* zone. The CaCO_3 content fluctuates with ~20% around a trend line that shifts from ~55% at the T–J transition to ~35% during the *A. liasicus* zone and gradually returns to ~50% in the upper Hettangian and lower Sinemurian (Fig. 5). Note that the (indurated) limestones are not included in the CaCO_3 record. A similar but opposite trend line is observed for the MS record. The large-scale fluctuations in the $\delta^{13}\text{C}_{\text{TOC}}$ and CaCO_3 records are concurrent and opposite to the TOC and MS records.

4.3. Frequency analysis

Spectral analysis was performed on the Hettangian and lower Sinemurian interval of the $\delta^{13}\text{C}_{\text{TOC}}$ record and the complete TOC and CaCO_3 datasets. Power spectra of the three proxy records show over ~90% significant spectral power, at ~3.5–4 m and at ~5.5–6 m (Fig. 6). A band-pass filter that includes both peaks in the power spectra indicates that these represent the larger meter-scale fluctuations observed in the proxy records and that they directly correspond to the limestone and shale-dominated bundles in lithology. The periodicity of oscillations in the proxy-filters varies directly with the variation in thickness of the bundles of limestone and black-shale predominance that are observed in the field (Fig. 5). Higher-frequency peaks in the power spectra are likely related to the occurrence of individual black-shales. These are however not filtered because of the too low resolution of the proxy records to properly resolve this cyclicity.

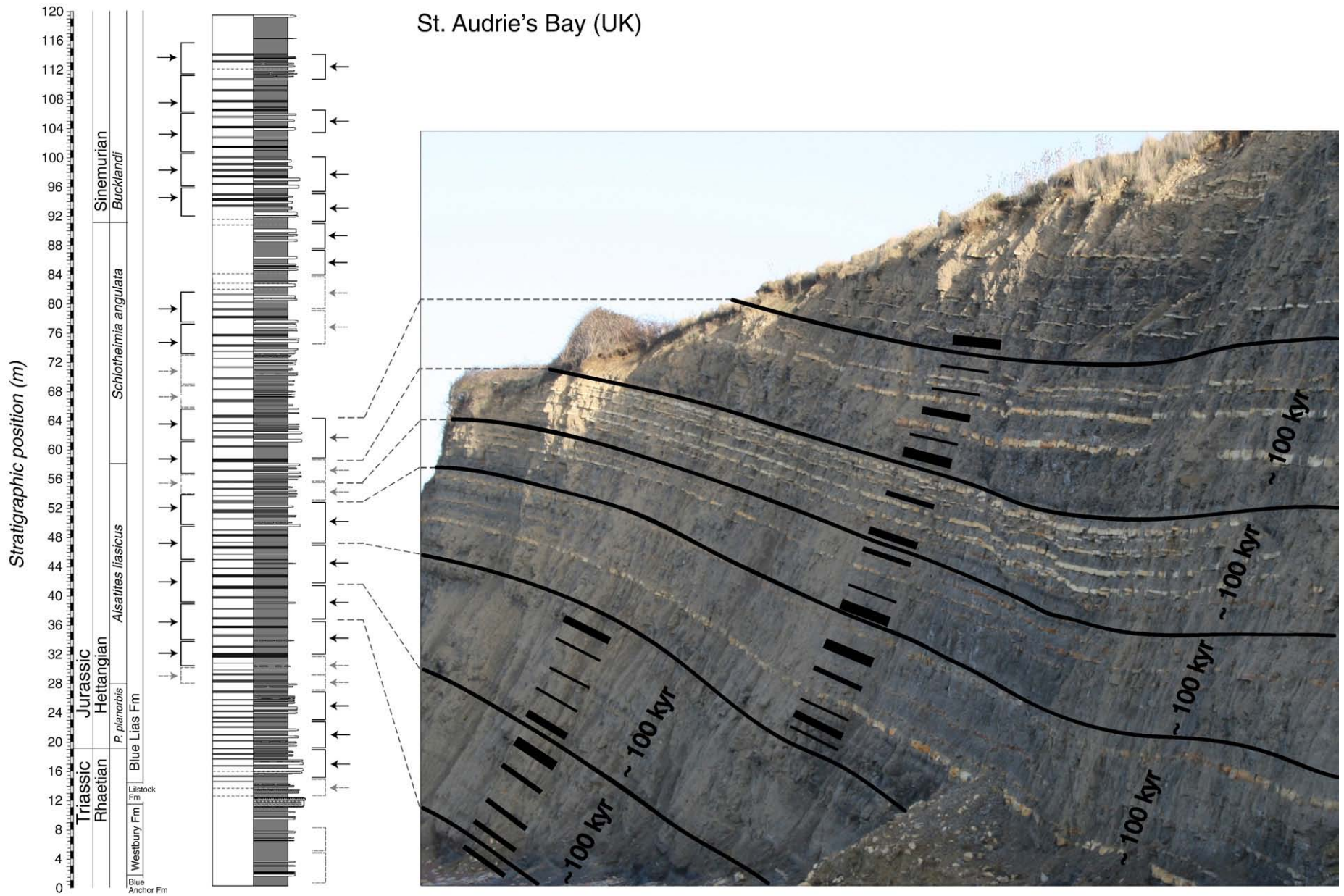


Fig. 4. Cliff-face overview of part of the Hettangian sedimentary sequence at St Audrie's Bay with corresponding lithological interval to the left (see Fig. 2). Continuous black lines reflect ~100-kyr eccentricity cycles (based on field observations and filtered proxy data). Black bars represent the stratigraphic position of black-shale horizons in the Hettangian *A. liasicus* and basal *S. angulata* ammonite zones in St Audrie's Bay.

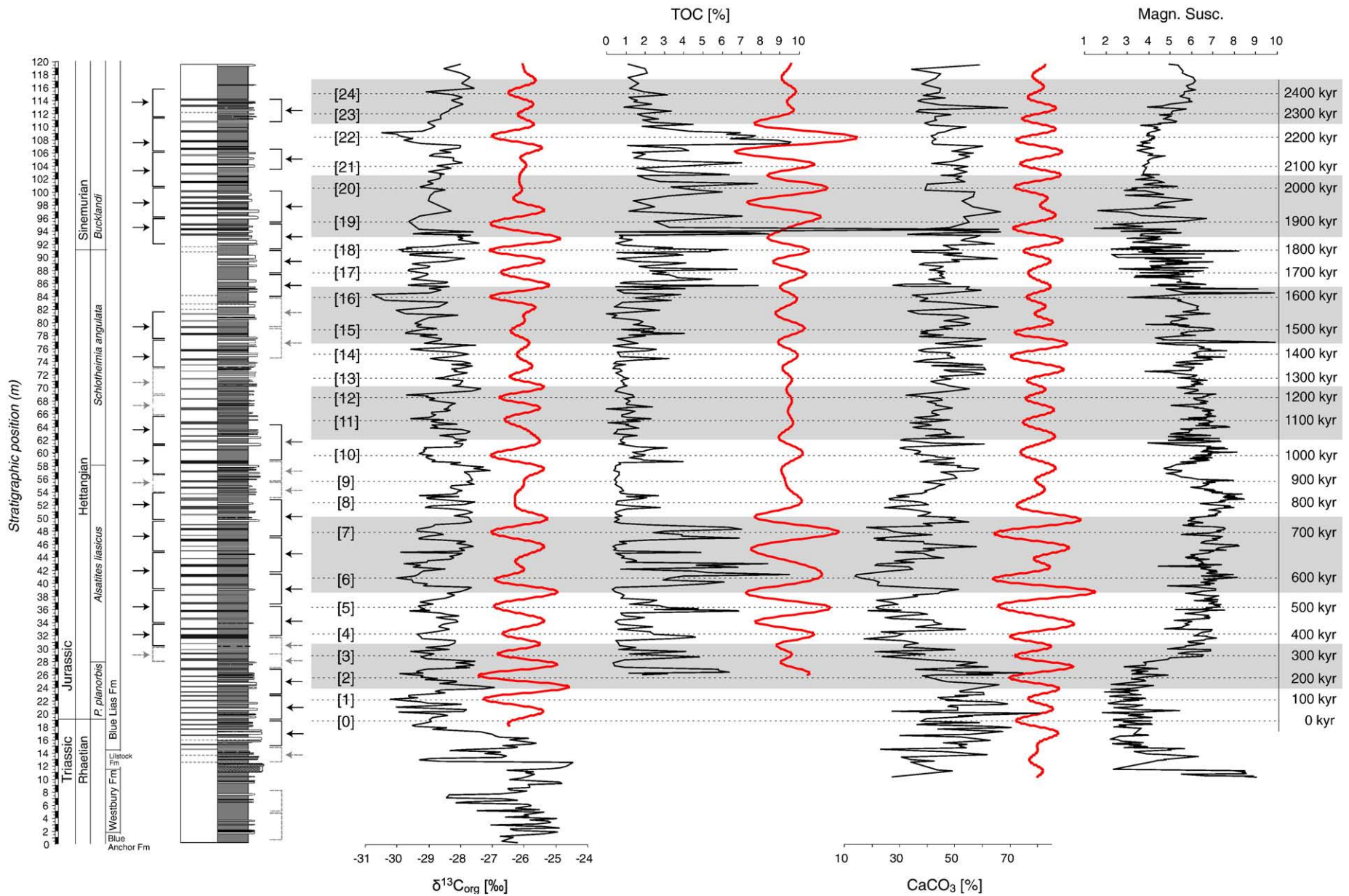


Fig. 5. The $\delta^{13}\text{C}_{\text{TOC}}$ [‰], TOC [%], CaCO_3 [%] and magnetic susceptibility proxy records, covering the upper Rhaetian to lower Sinemurian time interval. Red band-pass filters reflect ~ 100 -kyr eccentricity oscillations in the proxy records. The filters are based on two distinct peaks in the power spectra with a bandwidth of 263–727 cm for the $\delta^{13}\text{C}_{\text{TOC}}$ record, 306–788 cm for the TOC record and 286–669 cm for the CaCO_3 record. Grey shading represents tentatively assigned ~ 400 -kyr eccentricity cycles. Data from the first ~ 28.5 m of the $\delta^{13}\text{C}_{\text{TOC}}$ record is from Hesselbo et al. (2002). Numbers on the right of the lithological column represent the number of 100-kyr eccentricity cycles from the base of the Hettangian stage.

5. Discussion

5.1. Palaeo-environmental interpretation

Increased total organic carbon content during black-shale intervals concur with depleted $\delta^{13}\text{C}_{\text{TOC}}$ values. Terrestrial primary producers generally fractionate more strongly for ^{12}C relative to marine primary producers (Tyson, 1995; Killops and Killops, 2005). Depleted $\delta^{13}\text{C}$ values of the marine sedimentary organic matter could therefore suggest increased terrestrial organic matter influx as driver of fluctuations in the $\delta^{13}\text{C}_{\text{TOC}}$ signature (Fig. 5). Increased magnetic susceptibility values, related to higher siliciclastic sediment input, coincide with enriched TOC values and further suggest increased continental runoff. These patterns suggest that the formation of black-shales was likely related to an enhanced hydrological cycle, leading to increased runoff, increased supply of terrestrial organic matter and siliciclastics into the basin, a stratified water column and anoxic bottom water conditions (Bonis et al., in press). In this, we follow a similar interpretation for the Blue Lias succession as formulated by Weedon (1985/86).

Changes in monsoonal activity have immediate consequences for the magnitude of precipitation rates, runoff and weathering patterns (Crowley et al., 1992; Vollmer et al., 2008). Modelling studies by Kutzbach (1994) suggest ~ 23 -kyr precession cycle influence on rainfall and runoff over large parts of (sub-)tropical Pangaea, similar to the present-day low latitude African and Indian monsoon systems. Black-shale occurrence throughout the lower Jurassic of England is suggested to be controlled by precession-scale variations in insolation and increased monsoonal activity in this low latitude region (at approximately 26°N (Kent and Tauxe, 2005)). Global warming due to CAMP related CO_2 emissions (McElwain et al., 1999) and possible methane release from gas hydrates (Beerling and Berner, 2002) may have further enhanced the already large temperature gradient between the vast Pangaeon landmass and its surrounding oceans. It may have caused the landward expansion of atmospheric circulation patterns (Bonis et al., in press) and intensified monsoon activity (Crowley et al., 1992).

5.2. Astronomical forcing of lower Jurassic climate

The continuous presence of meter-scale sedimentary cycles in limestone and black-shale predominance, and their co-occurrence with cyclical patterns in the proxy records argues for a stable, allogenic forcing mechanism, likely to be astronomical forcing of Jurassic climate. Here, we argue that the occurrences of meter-scale lithological bundles are controlled by the ~ 100 -kyr eccentricity cycle, with an average of ~ 3.2 – 4.2 precession-controlled individual black-shale beds per bundle. The ratio of precession to short eccentricity is about 1 to 5 (~ 18 – 21.5 kyr to ~ 100 kyr) in early Jurassic times (Berger et al., 1992). In such an orbitally controlled system, not all individual precession cycles within an eccentricity cycle are expected to develop as black-shales. During eccentricity minima the amplitude of precession may be too low in order to cross the threshold for black-shale deposition. Neogene sapropel patterns deposited in the Mediterranean Sea for example, exhibit 2 to 5 sapropels for every ~ 100 -kyr eccentricity cycle. At times of prolonged eccentricity minima related to the 405-kyr cycle, sapropels lack or occur at 41-kyr obliquity frequency, reducing the amount of sapropels considerably (Hilgen et al., 2000; Hüsing et al., 2007). The individual black-shale to black-shale-bundle patterns observed in the Blue Lias Formation are thus in line with expected precession to short eccentricity forcing.

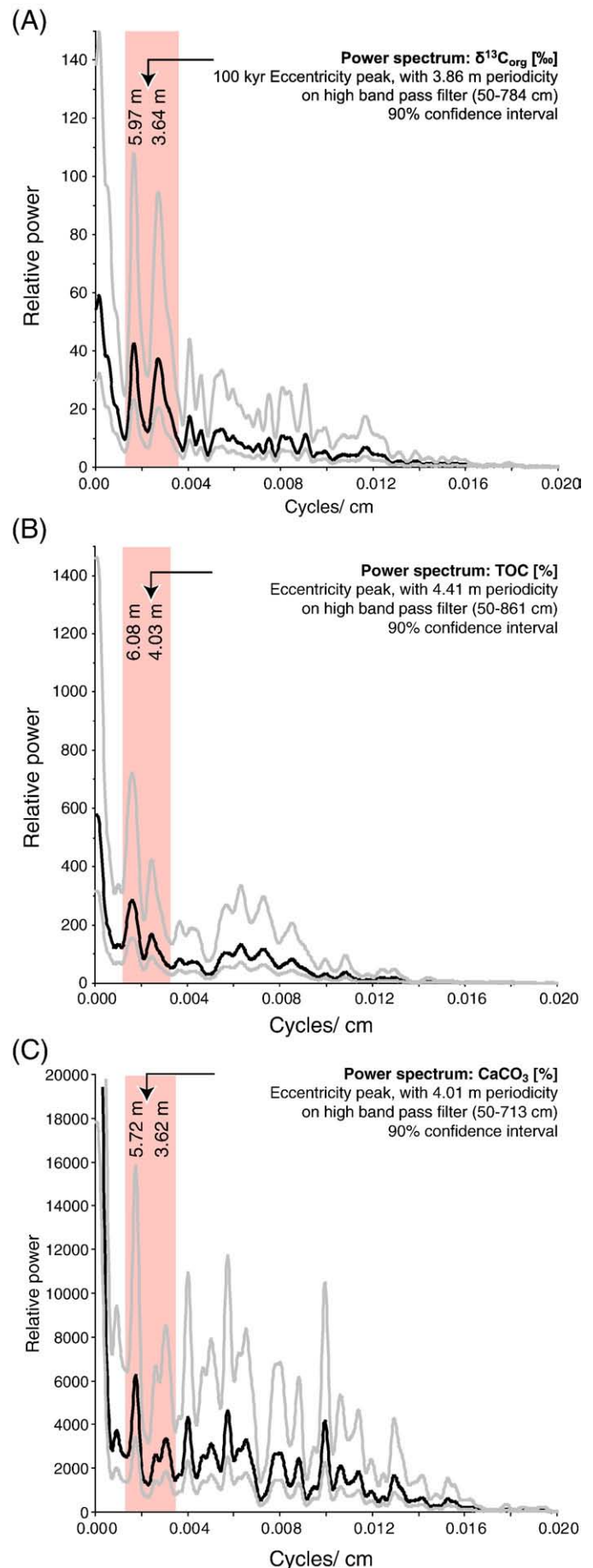


Fig. 6. Power spectra of time-series analysis of (A) the $\delta^{13}\text{C}_{\text{TOC}}$, (B) the total organic carbon and (C) the CaCO_3 proxy records. All three power spectra show main frequency peaks with an ~ 3.8 and ~ 5.8 m periodicity.

Eccentricity controlled middle–late Triassic climate oscillations have also been reported from older successions at St Audrie's Bay (Kemp and Coe, 2007), the mid-Germanic basin (Vollmer et al., 2008) and in the Newark basin (Olsen and Kent, 1996). Terrestrial climate response to 100-kyr eccentricity modulation of insolation can occur in low latitude land areas affected by fluctuations in monsoon intensity (Crowley et al., 1992). Orbitally controlled eccentricity cycles in palynofacies and organic and inorganic proxy records in the Jurassic of England typically cover four to five precession cycles (Van Buchem et al., 1994; Waterhouse, 1999a,b). Eccentricity-scale increases in marine and terrestrial palynomorph concentrations in the upper Triassic and lower Jurassic St Audrie's Bay sequence (Fig. 7 this study; Bonis et al., in press) coincide with low relative spore abundances and low magnetic susceptibility values (Fig. 5), further suggesting orbitally controlled fluctuations in the strength of the hydrological cycle.

Eccentricity strongly modulates the intensity of precession-scale climate forcing, especially visible in the organic proxy records (Fig. 5). A strongly enhanced hydrological cycle in concurrence with the negative CIE at the mass extinction interval is suggested by highly increased relative spore abundances with precession-scale fluctuations (Fig. 7). Wet phases in the lower Jurassic of St Audrie's Bay are likely enhanced during eccentricity maxima when the northern hemisphere summer resides in perihelion.

5.3. Cyclostratigraphic constraints on the duration of the Hettangian stage

The Hettangian stage in southwest England is, based on cyclostratigraphic interpretation of lithology, marked by 16 (but up to 20) bundles of limestone and black-shale predominance. These bundles are interpreted as ~100-kyr eccentricity cycles and suggest an ~1.6–2 Ma duration. However, the Hettangian stage is marked by 18 filtered oscillations in the chemical proxy-filters (Fig. 5). The potentially four observed limestone bundles in the middle of the *S. angulata* zone (bundles L13-a/b and L14-a/b) are clearly recognized in the filtered proxy records as two cycles (Fig. 5). Bundles L3-a/b and L8-a/b are marked by four oscillations in the filters. The 400-kyr eccentricity cycle, the most persistent eccentricity cycle over the past 200 Ma, is clearly recognized in the Newark basin (Olsen and Kent, 1996; Kent and Olsen, 1999). However, it is not well recognized in the north Somerset coastal sections of St Audrie's Bay and East Quantoxhead, similar to most of the Triassic in the Germanic basin (Bachmann and Kozur, 2004). Tentatively assigned 400-kyr cycles, based on tens of meter-scale oscillations in the chemical proxy records (Fig. 5), also suggest that the two sedimentary intervals with relatively short cycles (bundles L3-a,b and L8-a,b) should, rather than enhanced obliquity forcing during a long-term eccentricity minimum, also be considered as 100-kyr eccentricity cycles. We therefore consider a 1.8 Myr duration of the Hettangian stage in southwest England, as most feasible.

An earlier cyclostratigraphic study, based on periodic oscillations in magnetic susceptibility records of the Blue Lias Fm of Lyme Regis (Weedon et al., 1999), suggested orbitally controlled climate variations and a minimum duration of 1.29 Myr for the Hettangian stage. The Lyme Regis outcrop, however, is known to be marked by a significant hiatus in the top of the *S. angulata* zone (of about 50%) relative to the sedimentary sequences of St Audrie's Bay/East Quantoxhead and the Burton Row borehole (Smith, 1989). Correction of the estimated 1.29 Myr duration of the Hettangian stage of Weedon et al. (1999), using our cyclostratigraphically derived ~800-kyr duration of the *S. angulata* zone (Section 5.4), shows a remarkably similar result ($1.29 + 0.5 \times 0.8 = 1.69$ Myr) compared to our estimate of ~1.8 Myr. Previous estimates on the duration of the Hettangian stage, based on absolute radiometric dating techniques, varied significantly (Kent and Gradstein (1985): ~4 Myr; Haq et al. (1987; 1988): ~9 Myr; Gradstein et al. (2004): ~3.1 Myr). Our interpretation

of the duration of the Hettangian stage is however well within the error-margin of the most recent estimated duration of $\sim 2.05 \pm 0.57$ Myr (Schaltegger et al., 2008), which is based on radiometric U–Pb dating of zircons from volcanic ash layers from the Pucara group in the Utcubamba valley (northern Peru). Our results are also in line with a short duration of the Hettangian stage as proposed by Kent and Olsen (2008).

5.4. Cyclostratigraphic constraints on recovery rates and Hettangian ammonite zones

Biological and biogeochemical changes at the T–J transition have been extensively studied at St Audrie's Bay (Warrington et al., 2008 and references therein). The timing of recovery patterns is however poorly understood as no accurate chronostratigraphic framework is yet available. The first Jurassic *P. planorbis* ammonites in the St Audrie's Bay section occur ~6 m stratigraphically above the end-Triassic negative CIE (Hesselbo et al., 2002) and mark the base of the Hettangian stage in southwest England and the onset of post-extinction ecological recovery after the end-Triassic mass extinction.

Periodic variations in relative spore abundance may reflect precession-induced climate forcing in the late Triassic Lilstock Fm, suggesting an ~20–40 kyr duration of the end-Triassic negative CIE (Fig. 7) (Bonis et al., in press). Our cyclostratigraphic interpretations suggest that the FO of *P. planorbis* succeeds the end-Triassic negative CIE by 6 precession cycles (~120 kyr) (Fig. 7). The cyclostratigraphically constrained ~120-kyr duration of the end-Triassic ammonite gap (this study) is close to a recently estimated ~100-kyr duration, based on paleomagnetic and cyclostratigraphically constrained magnetic susceptibility data from northwest Europe and Morocco (Deenen et al., 2010).

Comparison of C-isotope and palynological records from St Audrie's Bay and the western Tethys Eiberg basin suggest an almost simultaneous FO of *C. thiergartii* pollen relative to an ~3.5‰ (main) negative shift in the uppermost Triassic (Ruhl et al., 2009; Bonis et al., 2010). The FO of *C. thiergartii* is closely succeeded (by only few meters) by the FO of *P. planorbis* and *P. spelaie* in St Audrie's Bay and the Eiberg basin, respectively. Consequently, these data suggest only a slightly younger age (of tens of kyr) for the first Jurassic ammonites in the northwest European sections compared to those in the western Tethys realm. It suggests a short duration for the *Tilmanni* Standard ammonite Zone (after Hillebrandt and Krystyn, 2009).

A similar duration for the end-Triassic ammonite gap is also estimated by Hillebrandt and Krystyn (2009). However, they suggest that the first Jurassic ammonite *P. planorbis* in the northwest European sections may be ~250 kyr younger than *P. spelaie*, the marker for the base of the Jurassic in the western Tethys realm. Their assumptions are based on estimated sedimentation rates in the latter region, rather than a concise and independent stratigraphic age model. Although a sedimentary hiatus or condensed interval could mark the basal Blue Lias Fm, previous palynological and C-isotope stratigraphical correlations between northwest Europe and the western Tethys Eiberg basin (Kürschner et al., 2007; Ruhl et al., 2009; Bonis et al., 2010) seem to be firm. A sedimentary break is also not observed in the field nor in any of the proxy records and is considered unlikely.

A previous study of Weedon (1985/86) assumed equal duration of Hettangian ammonite zones and suggested that variations in thickness of these biozones are largely controlled by changes in sedimentation rates. Our resolved orbitally-induced cycles in limestone and shale predominance and the periodic occurrence of black-shales throughout the Hettangian and lower Sinemurian strongly suggest relatively continuous sedimentation rates and consequently unequal durations of the Hettangian ammonite zones as suggested by Smith (1989). Our data suggests that the first Jurassic ammonite zone in St Audrie's Bay covers about 2.5 eccentricity cycles (~250 kyr) and is significantly shorter than the subsequent two Hettangian ammonite

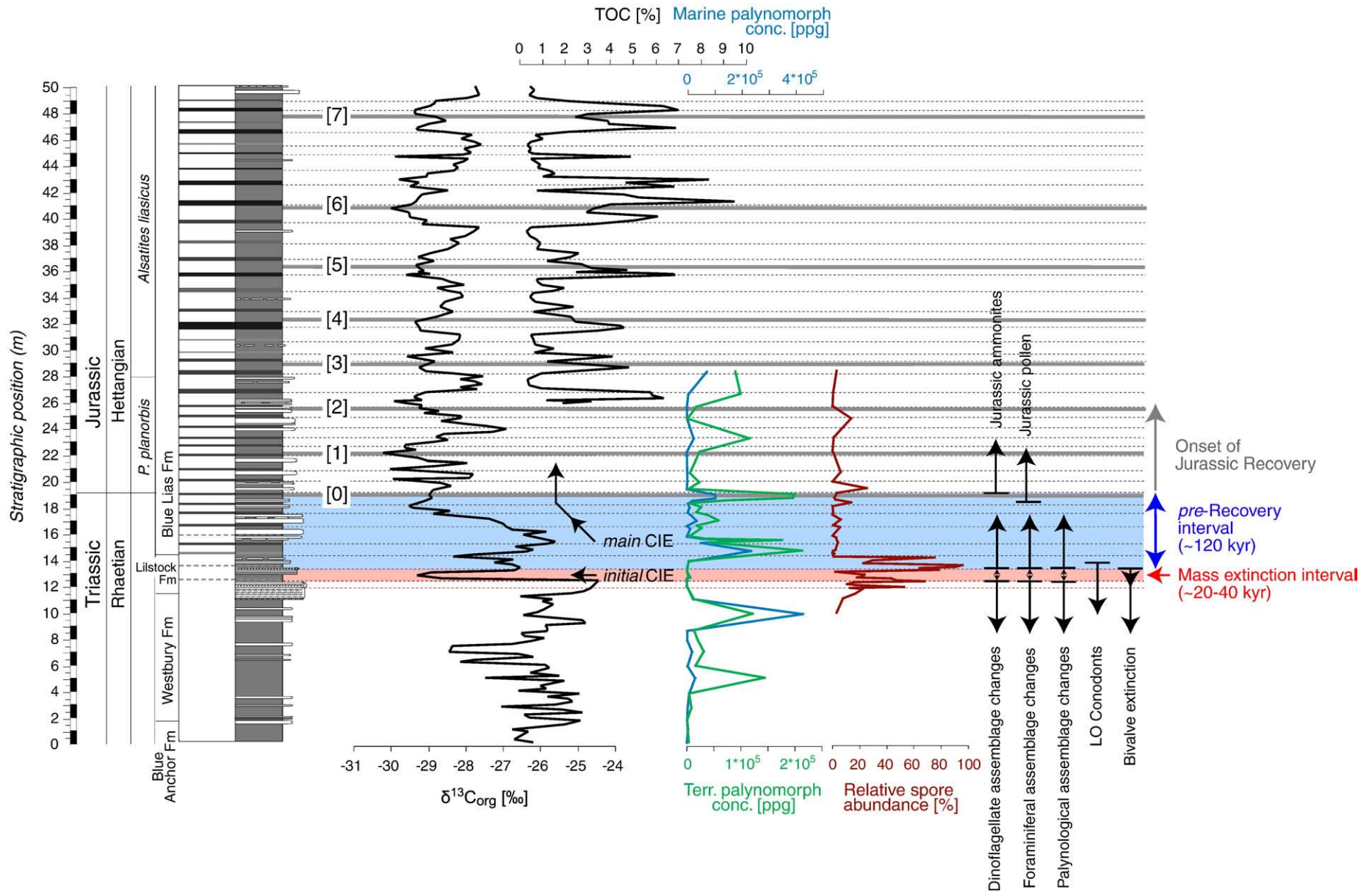


Fig. 7. The $\delta^{13}C_{TOC}$ [‰] and TOC [%] proxy records of St Audrie's Bay (with stratigraphic position in cm), relative to terrestrial (green curve) and marine (blue curve) palynomorph concentrations and relative spore abundance (red curve). First and last occurrences and marine and terrestrial assemblage changes are based on Warrington et al. (2008).

zones (*A. liasicus* zone: ~750 kyr and *S. angulata* zone: ~800 kyr). The shorter duration of the *P. planorbis* zone may be critically influenced by enhanced origination/mutation rates of earliest Jurassic ammonites caused by environmental stress during enhanced volcanic activity related to CAMP.

5.5. The lower Jurassic $\delta^{13}\text{C}_{\text{TOC}}$ record

The T–J transition interval is marked by two pronounced negative excursions in $\delta^{13}\text{C}_{\text{TOC}}$ records from several locations around the world (Pálffy et al., 2001; Guex et al., 2004; Galli et al., 2007; Ward et al., 2007; Ruhl et al., 2009). The St Audrie's Bay outcrop along the Somerset coast is marked by a short *initial* negative CIE of 5‰ that is separated from a succeeding and longer *main* negative CIE of 3.5‰ (Hesselbo et al., 2002). The *main* negative CIE in the $\delta^{13}\text{C}_{\text{TOC}}$ record coincides with a similarly shaped but smaller (~2‰) negative CIE in the $\delta^{13}\text{C}_{\text{CARB-Oyster}}$ record of the same section (Korte et al., 2009). Negative CIEs at the T–J boundary may therefore be regarded as actual recorders of global carbon cycle changes that are likely (in-)directly related to massive CO_2 release during CAMP volcanism (Hesselbo et al., 2002). The onset of end-Triassic volcanic activity in the Argana basin (Morocco) coincided with the *initial* negative CIE (Deenen et al., 2010). The onset of a major volcanic phase with emplacement of the intermediate unit in Morocco and the time-equivalent Orange Mt/Talcott basalts in the eastern USA, possibly precedes the onset of the *main* negative CIE (Deenen et al., 2010). The CAMP related basalt deposition in the Newark basin is, however, astronomically constrained to an ~600-kyr duration (Olsen et al., 2003; Whiteside et al., 2007). Volcanic activity and CAMP related CO_2 emissions may therefore be restricted to the lower Hettangian. Our extended $\delta^{13}\text{C}_{\text{TOC}}$ curve exhibits continuously low values throughout the Hettangian and early Sinemurian and prolongs the duration of the *main* CIE to over 2.3 Myr (Fig. 5). These data imply that either CAMP related volcanic activity lasted much longer than recorded in the continental basins of the eastern US, or that the $\delta^{13}\text{C}_{\text{TOC}}$ signature is not directly or only partly related to volcanic emissions. Although new species began to evolve already in the lower Hettangian, global biogeochemical cycles may have not fully recovered for several million years after the Triassic–Jurassic boundary, similar to delayed biogeochemical recovery following the Permian–Triassic (Payne and Kump, 2007; Galfetti et al., 2007) and Cretaceous–Paleogene mass extinctions (D'Hondt et al., 1998).

The ~2‰ fluctuations (with an ~3.8–5.8 m thickness) in the $\delta^{13}\text{C}_{\text{TOC}}$ record of St Audrie's Bay coincide with observed bundles in black-shale and limestone domination and are interpreted as ~100-kyr eccentricity controlled climate cycles.

Previous studies spanning the Hettangian and lower Sinemurian show a distinct positive excursion in the lower to middle Hettangian $\delta^{13}\text{C}_{\text{TOC}}$ (Williford et al., 2007) and bulk $\delta^{13}\text{C}_{\text{CARB}}$ (Van de Schootbrugge et al., 2008) records of the Kennecott Point (Queen Charlotte Islands, British Columbia, Canada) and Val Adrara (Italy) sections, respectively. The positive excursion in the latter section may be directly related to distinct changes in facies. A lower Jurassic positive excursion in the Kennecott Point section may be related to local ecological conditions and explained by increased marine primary productivity under high atmospheric CO_2 values, similar to the lower Triassic positive CIEs following the Permian–Triassic mass extinction (Payne and Kump, 2007).

5.6. Cyclostratigraphic constraints for correlation of the marine and continental realms

Late Triassic to lower Jurassic cyclostratigraphic time control is well established in the continental sequences of the Newark Supergroup (Kent and Olsen, 1999; Kent and Olsen, 2008). Orbitally controlled sedimentary cycles in these sections, mainly showing

precession and eccentricity forcing, mark one of the longest continuous sedimentary records available. Additional paleomagnetic studies resulted in a high resolution astronomically calibrated geomagnetic polarity time-scale of over 30 Myr (Kent and Olsen, 1999). This high resolution time frame constrained the duration of CAMP deposition in the eastern United States to ~580–610 (± 100) kyr (Olsen et al., 2003; Whiteside et al., 2007). Biostratigraphic time control in the Newark sequences is unfortunately hampered by the lack of age diagnostic fossils and provinciality of fossils. Several paleomagnetic correlations between the Newark and St Audrie's Bay sequences have been proposed (Hounslow et al., 2004; Knight et al., 2004; Whiteside et al., 2007; Marzoli et al., 2008; Deenen et al., 2010). Correlation of the extinction interval and negative CIE in St Audrie's Bay (Hesselbo et al., 2002) and the extinction interval marked by terrestrial ecosystem changes in the Newark basin (Olsen et al., 2002) is suggested by Deenen et al. (2010), with correlation of reversed polarity chron E23r in the Newark basin (Kent and Olsen, 1999) to reversed polarity intervals SA5n.2r and SA5n.3r in St Audrie's Bay (Hounslow et al., 2004). The data presented in this study may confirm their correlation as an ~5 cm/kyr sedimentation rate is suggested by cyclostratigraphy directly above SA5n.2r and SA5n.3r in St Audrie's Bay, suggesting a total ~30-kyr duration for this reversed polarity interval, almost similar to the ~26-kyr duration of E23r in the Newark Basin (Kent and Olsen, 1999). Additionally, the Newark cyclostratigraphic record is marked by a long-term eccentricity minimum, ~1.3 Ma after the extinction interval (Fig. 8) and reflected by poorly developed lake deposits in the continental sediment record. This long-term eccentricity minimum may also be reflected by poorly developed black-shale events in the marine realm of St Audrie's Bay, ~1.3 Ma after the marine extinction interval. However, this correlation implies that reversed polarity chron SA5n.1r in the UK, is not recorded or absent in the Newark sequence. It may represent a very short excursion of the normal paleomagnetic field, which is not resolved in the Newark basin or may be an artifact as it is based on one single sample of admitted poor paleomagnetic quality (Hounslow et al., 2004). Additionally, chron SA5r, although demonstrated for the Moroccan lava sequences (Knight et al., 2004), has yet not been recorded in the Newark sequence because of lower sampling resolution in the grey strata that characterizes the older parts of the syn-basalt sedimentary sequences.

Our cyclostratigraphic correlation of the marine St Audrie's Bay succession to the astronomically-tuned GPTS of the Newark basin is based on ~100-kyr eccentricity cycles observed in lithology and physical and chemical proxy records (Fig. 8). This correlation suggests that (i) the marine defined Triassic–Jurassic boundary is positioned between the Orange Mt/Talcott and Preakness/Holyoke basalts in the continental Newark and Hartford basins, respectively (Fig. 8). This position is supported by a recent palynological study in the Fundy basin (Cirilli et al., 2009). It also suggests that the marine defined base of the Sinemurian is positioned in the middle of the Mittingue Mb of the Hartford basin (eastern USA). It positions (ii) continentally deposited CAMP units in the marine stratigraphic record, with deposition of the Orange Mt and time-equivalent basalts of the eastern US coinciding with some negative $\delta^{13}\text{C}_{\text{TOC}}$ values, ~20 kyr after the *initial* negative CIE (Fig. 8). Deposition of the subsequent Preakness and Hook Mt time-equivalent basalts coincide with already low $\delta^{13}\text{C}_{\text{TOC}}$ values during the *main* CIE and diminished carbonate deposition in the marine record. The onset of volcanic activity and the possible release of methane from clathrates (Beerling and Berner, 2002) at the extinction interval possibly already initiated long-term changes in global biogeochemical cycles. Subsequent volcanic phases may therefore have been of lesser influence. It (iii) suggests the marine stratigraphic position of three observed reversed polarity chrons at the continental Hettangian–Sinemurian transition in the Hartford basin (Kent and Olsen, 2008). A short (~50 kyr) reversed polarity chron (Kent and Olsen, 2008) may be positioned in the

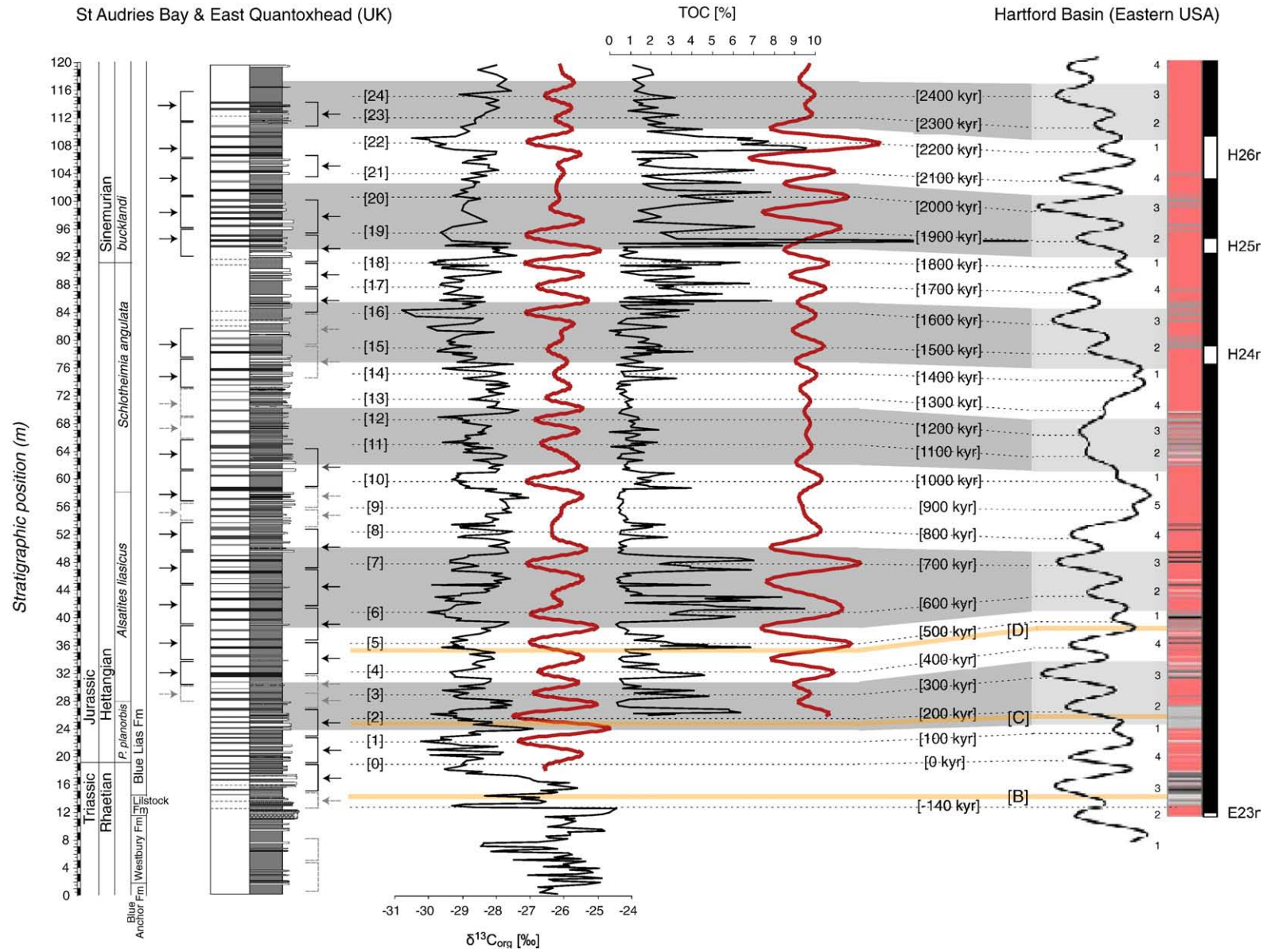


Fig. 8. Correlation of the ~100-kyr eccentricity filters of chemical proxy records in St Audrie's Bay/East Quantoxhead to the tuned lithology and eccentricity forced precession envelope of the Hartford basin (Kent and Olsen, 2008). Orange lines represent the stratigraphic position of [B] the Talcott/Orange Mt Basalt, [C] the Holyoke/Preakness Basalt and [D] the Hampden/Hook Mt Basalt in the Hartford basin and possible time-equivalent intervals in St Audrie's bay. Grey shading represents tentatively assigned ~400-kyr eccentricity cycles.

middle of the *S. angulata* ammonite zone and two subsequent reversed chrons in the lower *Bucklandi* zone of southwest England.

6. Conclusions

Combined field observations and proxy studies from the marine sedimentary sequence of St Audrie's Bay and East Quantoxhead demonstrate simultaneous fluctuations in black-shale and limestone predominance and chemical proxy records. Time-series analysis of the proxy records shows a main periodicity between ~3.8 and 5.8 m for these oscillations. Each oscillation is marked by ~3 to 5 black-shale horizons that are likely controlled by changes in monsoon intensity controlled by the precession cycle. The ~3.8–5.8-meter scale oscillations are interpreted as orbitally forced ~100-kyr eccentricity cycles. Our data constraints the duration of the Hettangian to 1.8 Myr. Lower Jurassic ammonite zones reveal to be unequal in duration, with the *P. planorbis* zone: ~250 kyr, the *A. liasicus* zone: ~750 kyr and the *S. angulata* zone: ~800 kyr. The end-Triassic mass extinction interval and coinciding negative CIE are possibly represented by 1–2 precession cycles (~20–40 kyr). The succeeding pre-recovery interval between the end-Triassic mass extinction and the first Jurassic ammonite occurrence is defined by 6 precession cycles (~120 kyr). Our cyclostratigraphic correlation of the St Audrie's Bay/East Quantoxhead succession to the astronomically-tuned GPTS of the Newark basin for the first time suggests the stratigraphic position of the continental equivalent of the marine defined T–J and Hettangian–Sinemurian boundary. The first would be positioned in between the Orange Mt and Preakness Basalt in the Newark basin and the latter would be located in the Mittinegue Mb of the Hartford basin (eastern USA). This correlation suggests no apparent influence of the CAMP related final volcanic phases on the $\delta^{13}\text{C}_{\text{TOC}}$ signature. The longer lasting negative carbon isotope excursion at the base of the Hettangian continues throughout the lower Jurassic and may reflect a shift to new long-term steady state values following CAMP volcanic activity in the lower Hettangian. Although new species began to evolve already in the lower Hettangian, Earth's biogeochemical cycles may have not fully recovered for several million years.

Acknowledgements

Dr. Mark Hounslow is gratefully acknowledged for excellent field guidance during the first fieldwork in the summer of 2007. A. van Dijk and T. Reichgelt are acknowledged for (assistance during) C-isotope measurements. This manuscript benefitted substantially from reviews by P.E. Olsen and D.V. Kent. This study is funded by the High Potential program of Utrecht University, The Netherlands. This is publication number 20100201 of The Netherlands research school of Sedimentary Geology (NSG).

Appendix A. Supplementary material

Supplementary data associated with this article can be found in the online version at doi:10.1016/j.epsl.2010.04.008.

References

- Bachmann, G., Kozur, H.W., 2004. The Germanic Triassic: correlations with the international chronostratigraphic scale, numerical ages and Milankovitch cyclicity. *Hallesches Jahrbuch Geowissenschaften* B26, 17–62.
- Bayer, U., 1987. Chronometric calibration of a comparative time-scale for the Mesozoic and Paleozoic. *Geol. Rundsch.* 76 (2), 485–503.
- Beerling, D.J., Berner, R.A., 2002. Biogeochemical constraints on the Triassic–Jurassic boundary carbon cycle event. *Global Biogeochem. Cycles* 16 (3).
- Berger, A., Loutre, M.F., Laskar, J., 1992. Stability of the astronomical frequencies over the Earth's history for paleoclimate studies. *Science* 255 (5044), 560–566.
- Bloos, G., Page, K.N., 2002. Global Stratotype Section and Point for base of the Sinemurian Stage (Lower Jurassic). *Episodes* 25 (1), 22–28.
- Bonis, N.R., Ruhl, M., Kürschner, W.M., 2010. Climate change driven black-shale deposition during the end-Triassic in the western Tethys. *Palaeogeography, Palaeoclimatology, Palaeoecology* 290, 151–159.
- Bonis, N.R., Ruhl, M., Kürschner, W.M., in press. Milankovitch-scale palynological turnover across the Triassic–Jurassic transition at St Audrie's Bay, SW UK. *Journal of the Geological Society, London*.
- Bottrell, S., Raiswell, R., 1989. Primary versus diagenetic origin of Blue Lias rhythms (Dorset, UK): evidence from sulphur geochemistry. *Terra Nova* 1, 451–456.
- Campos, H.S., Hallam, A., 1979. Diagenesis of English Lower Jurassic limestones as inferred from oxygen and carbon isotope analysis. *Earth Planet. Sci. Lett.* 45 (1), 23–31.
- Cirilli, S., Marzoli, A., Tanner, L., Bertrand, H., Buratti, N., Jourdan, F., Bellieni, G., Kontak, D., Renne, P.R., 2009. Latest Triassic onset of the Central Atlantic Magmatic Province (CAMP) volcanism in the Fundy Basin (Nova Scotia): new stratigraphic constraints. *Earth Planet. Sci. Lett.* 286 (3–4), 514–525.
- Crowley, T.J., Kim, K.Y., Mengel, J.G., Short, D.A., 1992. Modelling 100000-year climate fluctuations in pre-Pleistocene time-series. *Science* 255 (5045), 705–707.
- Deconinck, J.-F., Hesselbo, S.P., Debuissier, N., Averbuch, O., Baudin, F., Bessa, J., 2003. Environmental controls on clay mineralogy of an Early Jurassic mudrock (Blue Lias Formation, southern England). *Int. J. Earth Sci. (Geol. Rundsch.)* 92, 255–266.
- Deenen, M.H.L., Ruhl, M., Bonis, N.R., Krijgsman, W., Kürschner, W.M., Reitsma, M., Van Bergen, M.J., 2010. A new chronology for the end-Triassic mass extinction. *Earth Planet. Sci. Lett.* 291, 113–125.
- D'Hondt, S., Donaghay, P., Zachos, J.C., Luttenberg, D., Lindinger, M., 1998. Organic carbon fluxes and ecological recovery from the Cretaceous–Tertiary mass extinction. *Science* 282, 276–279.
- Galfetti, T., Bucher, H., Ovtcharova, M., Schaltegger, U., Brayard, A., Bruehwiler, T., Goudemand, N., Weissert, H., Hochuli, P.A., Cordey, F., Guodun, K., 2007. Timing of the early Triassic carbon cycle perturbations inferred from new U–Pb ages and ammonoid biochronozones. *Earth Planet. Sci. Lett.* 258, 593–604.
- Galli, M.T., Jadoui, F., Bernasconi, S.M., Cirilli, S., Weissert, H., 2007. Stratigraphy and palaeoenvironmental analysis of the Triassic–Jurassic transition in the western Southern Alps (Northern Italy). *Palaeogeogr. Palaeoclimatol. Palaeoecol.* 244, 52–70.
- Gradstein, F.M., Ogg, J.G., Smith, A.G., Bleeker, W., Lourens, L.J., 2004. A new Geologic Time Scale, with special reference to Precambrian and Neogene. *Episodes* 27 (2), 83–100.
- Guex, J., Bartolini, A., Atudorei, V., Taylor, D., 2004. High-resolution ammonite and carbon isotope stratigraphy across the Triassic–Jurassic boundary at New York Canyon (Nevada). *Earth Planet. Sci. Lett.* 225 (1–2), 29–41.
- Hallam, A., 1986. Origin of minor limestone-shale cycles: climatically induced or diagenetic? *Geology* 14 (7), 609–612.
- Hallam, A., 1987. Radiations and extinctions in relation to environmental change in the Marine Lower Jurassic of Northwest Europe. *Paleobiology* 13 (2), 152–168.
- Hallam, A., 1995. Oxygen restricted facies of the basal Jurassic of north-west Europe. *Hist. Biol.* 10, 247–257.
- Hallam, A., 1997. Estimates of the amount and rate of sea-level change across the Rhaetian–Hettangian and Pliensbachian–Toarcian boundaries (latest Triassic to early Jurassic). *J. Geol. Soc.* 154, 773–779.
- Hallam, A., Wignall, P.B., 1999. Mass extinctions and sea-level changes. *Earth Sci. Rev.* 48 (4), 217–250.
- Haq, B.U., Hardenbol, J., Vail, P.R., 1987. Chronology of fluctuating sea levels since the Triassic. *Science* 235 (4793), 1156–1167.
- Haq, B.U., Hardenbol, J., Vail, P.R., 1988. Mesozoic and Cenozoic chronostratigraphy and cycles of sea-level change. *Sea-level Changes: An Integrated Approach*, pp. 71–108.
- Hesselbo, S.P., Robinson, S.A., Surlyk, F., Piasecki, S., 2002. Terrestrial and marine extinction at the Triassic–Jurassic boundary synchronized with major carbon-cycle perturbation: a link to initiation of massive volcanism? *Geology* 30 (3), 251–254.
- Hesselbo, S.P., Robinson, S.A., Surlyk, F., 2004. Sea-level change and facies development across potential Triassic–Jurassic boundary horizons, SW Britain. *J. Geol. Soc.* 161, 365–379.
- Hilgen, F.J., Krijgsman, W., Raffi, I., Turco, E., Zachariasse, W.J., 2000. Integrated stratigraphic and astronomical calibration of the Serravallian/Tortonion boundary section at Monte Gibliscemi (Sicily, Italy). *Mar. Micropaleontol.* 38, 181–211.
- Hillebrandt, A.V., Krystyn, L., 2009. On the oldest Jurassic ammonites of Europe (Northern Calcareous Alps, Austria) and their global significance. *N. Jb. Geol. Palaeont. Abh.* 253, 163–195.
- Hillebrandt, A.V., Krystyn, L., Kürschner, W.M., 2007. A candidate GSSP for the base of the Jurassic in the Northern Calcareous Alps (Kuhjoch section, Karwendel Mountains, Tyrol, Austria). *International Subcommittee on Jurassic Stratigraphy Newsletter* 34 (1), 2–20.
- Hounslow, M.W., Posen, P.E., Warrington, G., 2004. Magnetostratigraphy and biostratigraphy of the upper Triassic and lowermost Jurassic succession, St Audrie's Bay, UK. *Palaeogeogr. Palaeoclimatol. Palaeoecol.* 213 (3–4), 331–358.
- Hüsing, S.K., Hilgen, F.J., Abdul Aziz, H., Krijgsman, W., 2007. Completing the Neogene geological time scale between 8.5 and 12.5 Ma. *Earth Planet. Sci. Lett.* 253, 340–358. doi:10.1016/j.epsl.2006.10.036.
- Kemp, D.B., Coe, A.L., 2007. A non-marine record of eccentricity forcing through the upper Triassic of south-west England and its correlation with the Newark basin astronomically calibrated geomagnetic polarity time scale from North America. *Geology* 35 (11), 991–994.
- Kent, D.V., Gradstein, F.M., 1985. A Cretaceous and Jurassic geochronology. *Geol. Soc. Am. Bull.* 96 (11), 1419–1427.
- Kent, D.V., Olsen, P.E., 1999. Astronomically tuned geomagnetic polarity time scale for the Late Triassic. *J. Geophys. Res.* 104 (B6), 12,831–12,841.
- Kent, D.V., Olsen, P.E., 2008. Early Jurassic magnetostratigraphy and paleolatitudes from the Hartford continental rift basin (eastern North America): testing for polarity bias

- and abrupt polar wander in association with the central Atlantic magmatic province. *J. Geophys. Res.* 113.
- Kent, D.V., Tauxe, L., 2005. Corrected late Triassic latitudes for continents adjacent to the North Atlantic. *Science* 307 (5707), 240–244.
- Killops, S., Killops, V., 2005. *Introduction to Organic Geochemistry*, 2nd Edition. Blackwell Publishing.
- Knight, K.B., Nomade, S., Renne, P.R., Marzoli, A., Bertrand, H., Youbi, N., 2004. The Central Atlantic Magmatic Province at the Triassic–Jurassic boundary: paleomagnetic and $^{40}\text{Ar}/^{39}\text{Ar}$ evidence from Morocco for brief, episodic volcanism. *Earth Planet. Sci. Lett.* 228 (1–2), 143–160.
- Korte, C., Hesselbo, S.P., Jenkyns, H.C., Rickaby, R.E.M., Spotl, C., 2009. Palaeoenvironmental significance of carbon- and oxygen-isotope stratigraphy of marine Triassic–Jurassic boundary sections in SW Britain. *J. Geol. Soc.* 166 (3), 431–445.
- Kürschner, W.M., Bonis, N.R., Krystyn, L., 2007. Carbon-isotope stratigraphy and palynostratigraphy of the Triassic–Jurassic transition in the Tiefengraben section – Northern Calcareous Alps (Austria). *Palaeogeography, Palaeoclimatology, Palaeoecology* 244 (1–4), 257–280.
- Kutzbach, J.E., 1994. Idealized Pangean climates: sensitivity to orbital change. In: Klein, G.D. (Ed.), *Pangea: Paleoclimate, Tectonics, and Sedimentation during Accretion, Zenith, and Breakup of a Supercontinent: Boulder, Colorado*, 288, pp. 41–55.
- Mander, L., Twitchett, R.J., 2008. Quality of the Triassic–Jurassic bivalve fossil record in north-west Europe. *Palaeontology* 51 (6), 1213–1223.
- Mander, L., Twitchett, R.J., Benton, M.J., 2008. Palaeoecology of the late Triassic extinction event in the SW UK. *J. Geol. Soc.* 165 (1), 319–332.
- Marzoli, A., Bertrand, H., Knight, K.B., Cirilli, S., Buratti, N., Verati, C., Nomade, S., Renne, P.R., Youbi, N., Martini, R., Allenbach, K., Neuwerth, R., Rapaille, C., Zaninetti, L., Bellieni, G., 2004. Synchrony of the Central Atlantic magmatic province and the Triassic–Jurassic boundary climatic and biotic crisis. *Geology* 32 (11), 973–976.
- Marzoli, A., Bertrand, H., Knight, K.B., Cirilli, S., Nomade, S., Renne, P.R., Verati, C., Youbi, N., Martini, R., Bellieni, G., 2008. Comment on “Synchrony between the Central Atlantic magmatic province and the Triassic–Jurassic mass-extinction event? By Whiteside et al. (2007)”. *Palaeogeogr. Palaeoclimatol. Palaeoecol.* 262 (3–4), 189–193.
- McElwain, J.C., Beerling, D.J., Woodward, F.I., 1999. Fossil plants and global warming at the Triassic–Jurassic boundary. *Science* 285 (5432), 1386–1390.
- McElwain, J.C., Wagner, P.J., Hesselbo, S.P., 2009. Fossil plant relative abundances indicate sudden loss of Late Triassic biodiversity in East Greenland. *Science* 324, 1554–1556.
- McRoberts, C.A., Newton, C.R., 1995. Selective extinction among end-Triassic European bivalves. *Geology* 23 (2), 102–104.
- Morton, N., 2008a. Selection and voting procedures for the base Hettangian. *International Subcommission on Jurassic Stratigraphy, Newsletter* 35 (1), 67.
- Morton, N., 2008b. Details of voting on proposed GSSP and ASSP for the base Hettangian Stage and Jurassic System. *International Subcommission on Jurassic Stratigraphy, Newsletter* 35 (1), 74.
- Olsen, P.E., Kent, D.V., 1996. Milankovitch climate forcing in the tropics of Pangea during the late Triassic. *Palaeogeogr. Palaeoclimatol. Palaeoecol.* 122 (1–4), 1–26.
- Olsen, P.E., Kent, D.V., Sues, H.-D., Koeberl, C., Huber, H., Montanari, A., Rainforth, E.C., Fowell, S.J., Szajna, M.J., Hartline, B.W., 2002. Ascent of dinosaurs linked to an Iridium anomaly at the Triassic–Jurassic boundary. *Science* 296, 1305–1307.
- Olsen, P.E., Kent, D.V., Et-Touhami, M., Puffer, J., 2003. Cyclo-, magneto-, and biostratigraphic constraints on the duration of the CAMP event and its relationship to the Triassic–Jurassic boundary. *Geophys. Monogr.* 136, 7–32 The Central Atlantic Magmatic Province: Insights from Fragments of Pangea. *American Geophysical Union*.
- Paillard, D.L., Labeyrie, M.A., Yiou, P., 1996. Macintosh program performs time-series analysis. *EOS Trans. AGU* 77, 379.
- Pálffy, J., 2008. The quest for refined calibration of the Jurassic time-scale. *Proc. Geol. Assoc.* 119, 85–95.
- Pálffy, J., Smith, P.L., Mortensen, J.K., 2000. A U–Pb and $^{40}\text{Ar}/^{39}\text{Ar}$ time scale for the Jurassic. *Can. J. Earth Sci.* 37, 923–944.
- Pálffy, J., Demeny, A., Haas, J., Hetenyi, M., Orchard, M.J., Veto, I., 2001. Carbon isotope anomaly and other geochemical changes at the Triassic–Jurassic boundary from a marine section in Hungary. *Geology* 29 (11), 1047–1050.
- Paul, C.R.C., Allison, P.A., Brett, C.E., 2008. The occurrence and preservation of ammonites in the Blue Lias Formation (lower Jurassic) of Devon and Dorset, England and their palaeoecological, sedimentological and diagenetic significance. *Palaeogeogr. Palaeoclimatol. Palaeoecol.* 270 (3–4), 258–272.
- Payne, J.L., Kump, L.R., 2007. Evidence for recurrent early Triassic massive volcanism from quantitative interpretation of carbon isotope fluctuations. *Earth Planet. Sci. Lett.* 256 (1–2), 264–277.
- Radley, J.D., 2008. Seafloor erosion and sea-level change: Early Jurassic Blue Lias Formation of central England. *Palaeogeogr. Palaeoclimatol. Palaeoecol.* 270, 287–294.
- Raup, D.M., Sepkoski, J.J., 1982. Mass extinctions in the marine fossil record. *Science* 215 (4539), 1501–1503.
- Ruhl, M., Kürschner, W.M., Krystyn, L., 2009. Triassic–Jurassic organic carbon isotope stratigraphy of key sections in the western Tethys realm (Austria). *Earth Planet. Sci. Lett.* 281 (3–4), 169–187.
- Schaltegger, U., Guex, J., Bartolini, A., Schoene, B., Ovtcharova, M., 2008. Precise U–Pb age constraints for end-Triassic mass extinction, its correlation to volcanism and Hettangian post-extinction recovery. *Earth Planet. Sci. Lett.* 267 (1–2), 266–275.
- Schoene, B., Crowley, J.L., Condon, D.J., Schmitz, M.D., Bowring, S.A., 2006. Re-assessing the uranium decay constants for geochronology using ID-TIMS U–Pb data. *Geochim. Cosmochim. Acta* 70 (2), 426–445.
- Smith, D.G., 1989. Stratigraphic correlation of presumed Milankovitch cycles in the Blue Lias (Hettangian to earliest Sinemurian), England. *Terra Nova* 1, 457–460.
- Tyson, R.V., 1995. *Sedimentary Organic Matter: Organic Facies and Palynofacies*. Chapman & Hall, London.
- Van Buchem, F.S.P., McCave, I.N., Weedon, G.P., 1994. Orbitally induced small-scale cyclicity in a siliciclastic epicontinental setting (Lower Lias, Yorkshire, UK). *Spec. Publ. Int. Assoc. Sedimentol.* 19, 345–366.
- Van de Schootbrugge, B., et al., 2008. Carbon cycle perturbation and stabilization in the wake of the Triassic–Jurassic boundary mass-extinction event. *Geochim. Geophys. Geost. J.* 9 (1). doi:10.1029/2007GC001914.
- Van Hinte, J.E., 1976. Jurassic time scale. *AAPG Bull.* 60 (4), 489–497.
- Vollmer, T., Werner, R., Weber, M., Tougiannidis, N., Röhling, H.-G., Hambach, U., 2008. Orbital control on Upper Triassic Playa cycles of the Steinmergel-Keuper (Norian): a new concept for ancient playa cycles. *Palaeogeogr. Palaeoclimatol. Palaeoecol.* 267 (1–2), 1–16.
- Ward, P.D., Garrison, G.H., Williford, K.H., Kring, D.A., Goodwin, D., Beattie, M.J., McRoberts, C.A., 2007. The organic carbon isotopic and paleontological record across the Triassic–Jurassic boundary at the candidate GSSP section at Ferguson Hill, Muller Canyon, Nevada, USA. *Palaeogeogr. Palaeoclimatol. Palaeoecol.* 244 (1–4), 281–289.
- Warrington, G., Cope, J.C.W., Ivimey-Cook, H.C., 1994. St-Audries Bay, Somerset, England – a candidate Global Stratotype Section and Point for the base of the Jurassic System. *Geol. Mag.* 131 (2), 191–200.
- Warrington, G., Cope, J.C.W., Ivimey-Cook, H.C., 2008. The St Audrie's Bay – Doniford Bay section, Somerset, England: updated proposal for a candidate Global Stratotype Section and Point for the base of the Hettangian Stage, and of the Jurassic System. *International Subcommission on Jurassic Stratigraphy Newsletter* 35 (1), 2–66.
- Waterhouse, H.K., 1999a. Orbital forcing of palynofacies in the Jurassic of France and the United Kingdom. *Geology* 27, 511–514.
- Waterhouse, H.K., 1999b. Regular terrestrially derived palynofacies cycles in irregular marine sedimentary cycles, Lower Lias, Dorset, UK. *J. Geol. Soc. London* 156, 1113–1124.
- Weedon, G.P., 1985/86. Hemi-pelagic shelf sedimentation and climatic cycles: the basal Jurassic (Blue Lias) of South Britain. *Earth Planet. Sci. Lett.* 76 (3–4), 321–335.
- Weedon, G.P., Jenkyns, H.C., Coe, A.L., Hesselbo, S.P., 1999. Astronomical calibration of the Jurassic time-scale from cyclostratigraphy in British mudrock formations. *Philos. Trans. R. Soc. Lond.* 357, 1787–1813.
- Whiteside, J.H., Olsen, P.E., Kent, D.V., Fowell, S.J., Et-Touhami, M., 2007. Synchrony between the Central Atlantic Magmatic Province and the Triassic–Jurassic mass-extinction event? *Palaeogeogr. Palaeoclimatol. Palaeoecol.* 244 (1–4), 345–367.
- Whittaker, A., Green, G.W., 1983. *Geology of the country around Weston-Super-Mare*. Memoirs of the Geological Survey of Great Britain, p. 279.
- Wignall, P.B., Bond, D.P.G., 2008. The end-Triassic and early Jurassic mass extinction records in the British Isles. *Proc. Geol. Assoc.* 119, 73–84.
- Williford, K.H., Ward, P.D., Garrison, G.H., Buick, R., 2007. An extended organic carbon-isotope record across the Triassic–Jurassic boundary in the Queen Charlotte Islands, British Columbia, Canada. *Palaeogeogr. Palaeoclimatol. Palaeoecol.* 244, 290–296.
- Yang, Z., Moreau, M.-G., Bucher, H., Dommergues, J.-L., Trouiller, A., 1996. Hettangian and Sinemurian magnetostratigraphy from the Paris Basin. *J. Geophys. Res. B: Solid Earth* 101 (4), 8025–8042.